International Journal of Engineering Applied Sciences and Technology, 2021
Vol. 6, Issue 6, ISSN No. 2455-2143, Pages 22-30
Published Online October 2021 in IJEAST (http://www.ijeast.com)

A COMPARISON STUDY ON MICRO-BULGING AND SHORTLESS PEENING PROCESSES USING WATER JET CAVITATION

James Kwasi Quaisie[1*], Philip Yamba[1], Joseph Sekyi-Ansah[2], Anthony Akayeti[1], Samuel Boakye[3].
[1]Faculty of Engineering (Welding and Fabrication Department), Tamale Technical University, Tamale, 00233, Ghana
[2] Department of Mechanical Engineering, Takoradi Technical University, Takoradi, 00233, Ghana
[3] Department of Agriculture Science, Sefwi Wiawso Senior High School, Sefwi Wiawso, 00233, Ghana

Abstract - This paper presents a comparative study using a newly technology called water jets cavitation to fabricate micro feature on 304 stainless steel foils with a thickness of 100 µm and surface enhancement of 8090Al-Li alloy sample with a thickness of 4 mm, where angular nozzle and a designed cavitation system were used with an incident pressure of 8-20 MPa. The bulged sample and the effect of incident pressure on the cavitation zone range were investigated. The experimental results indicated that the formed sample bulging depth of the outer ring shock zone and the bulging depth of the jet shock zone were not ideal, while the pits in the cavitation shock zone (that is, pits 2~4 and 10~12) obtained good geometric characteristics. Finally, the consistency of the maximum bulging depth was relatively good. The micro-bulged parts showed that the micro-pits in the cavitation shock zone had a large bulging depth and their uniformity was relatively good, indicating that the circular array feature micro-die has good performance in the cavitation water jet shock micro-bulging process. The effect of incident pressure on the range of cavitation zone, also indicated that the effective area of action of the cavitation water jet showed a ring. That is when the incident pressure was 20 MPa with a target distance of 120 mm, the maximum cavitation shock (bulging) zone showed rings of 3.5 〜21.1 mm with the 304 stainless steel foil and 3.5 mm~21.4 mm also with the 8090Al-Li alloy plate which were approximately same.

Keywords*: Water jets cavitation, Micro-bulging, Cavitation nozzle, Cavitation zone range, Plastic deformation, shortless peening.*

I. INTRODUCTION

The trend in miniaturization of micro metal parts has been extensively used in the engineering field, such as micro-systems technologies (MST), electrical and electronic devices (EED), and microelectromechanical-systems (MEMS) [1]. Micro-forming technology has recently attracted more attention in microfabrication technologies mainly because of the advantages it gives, such as low rate of material waste, excellent mechanical properties, and high productivity, as compared to other micro-manufacturing technologies including the micromachining and lithographic techniques [2]. Micro forming is a prominent micro-manufacturing method for producing very small metallic components in the submillimeter range, and a variety of micro forming technologies have been developed over the years to manufacture a wide range of micro products with a variety of uses [3]. The microforming using metallic foil becoming more focused on current research, and this micro forming of foils include micro bending, micro drawing, and micro bulging [4].

Over the years most studies have been conducted using various forms of technology for the production of micro-parts and surface strengthening. Wang et al. [2] investigated micro hydraulic bulging using laser shock on copper foil. The formed depth and roughness of the surface increased with the laser energy, according to the results. However, as the laser energy was raised, the surface roughness rose marginally, and no thermal response area was identified at the forming area. When laser energies of 565, 835, and 1200 mJ were used, the fillet region obtained the maximum thickness thinning, whereas fracture occurred in the bottom region (not the apex) as the energy of the laser was increased to 1380 mJ. Using electro-magnetic bulging, Liu et al. [5] studied into a new laser shock hydroforming method for micro-tube bulging. The dynamic forming process of micro tubes was initially investigated numerically, with numerical results agreeing with experimental findings. The results indicated that the homogeneity of the thickness distribution improved as compared to the condition of quasi-static, and the improvement was examined numerically. Quaisie et al. [6] investigated the water-jet shock microforming process utilizing a variety of incidence pressures. The testing results showed that under this dynamic microforming approach, the surface morphology of the metallic foils achieved good geometrical features and that there were no cracks or fractures. With increasing incident pressure, the formed

International Journal of Engineering Applied Sciences and Technology, 2021
Vol. 6, Issue 6, ISSN No. 2455-2143, Pages 22-30
Published Online October 2021 in IJEAST (http://www.ijeast.com)

depth and surface roughness increased. At an incident pressure of 8 MPa to 20 MPa, the formed depth increased from 124.7 m to 327.8 m, while the roughness of the surface increased from 0.685 m to 1.159 m. Sekyi-Ansah et al. [7] used 8090AL-Li Alloy to investigate the cavitation damage and surface features using water jet peening technique, the results confirmed that the effect of the cavitation occurred in the collapsed zone. Using Al alloy 5052 ultra-thin sheet, Wang et al. [8] utilized an ultrasonic flexible bulging approach of spherical caps array as surface texturing utilizing Al 5052 alloy ultra-thin sheet. The ultrasonic flexible bulging improves the surface quality and increases the height of the bulged cap and the length of the intersection edge, according to the results of the experiments. Wu et al. [9] investigated a unique 3D deformation measurement technique for micro-scale bulge-testing under an optical microscope. The experimental results suggested that the proposed technology and the bulge-test apparatus may be used to successfully characterize the films thermal/mechanical properties of the micro-scale. Water jet cavitation peening (WCP) uses cavitation induced by a shear layer generated by dual concentric co-flowing jets with a considerable velocity difference to introduce compressive residual stresses in the surface layers of metal components subjected to fatigue loading or corrosive environments [10]. Soyama [11] made comparative analysis on the effects of water jet peening, cavitation peening, laser peening and shot peening on the fatigue strength of stainless steel. The optimum coverage for each peening procedure was determined by testing the fatigue life under constant bending load. The fatigue strength of treated samples with the best coverage was then investigated. The non-peened specimen had a fatigue strength of 279 MPa, whereas cavitation peening had a fatigue strength of 348 MPa, shot peening had a fatigue strength of 325 MPa, laser peening had a fatigue strength of 303 MPa, and water jet peening had a fatigue strength of 296 MPa. Surface roughness and work hardening had an impact on the fatigue strength of each peening process. Macron [12] utilized Al 7075-T651 to study the nozzle size scaling impact in co-flow cavitating water jet peening. The results reveal a significant rise in cavitation intensity as nozzle size increases, as well as a significant reduction in the processing time required for strip curvature saturation and residual stress. This study on focuses much on the micro-bulging and shortless peening process using water jet cavitation for the plastic deformation. This work investigates the newly water jet cavitation shock micro bulging and surface strengthening techniques. 304 stainless steel foil and aluminums lithium 8090 alloy plate were selected to study the impact of incident pressure on the surface of forming sample and the cavitation zone range.

II. FORMING MECHANISM OF WATER JET CAVITATION SHOCK MICRO-BULGING (FORMING)

Figure 1 shows the forming mechanism of micro bulging using water-jet cavitation shock. In this section, the foil was placed on the top of the die, covering the die-openings completely. Then the cavitation bubbles are generated by injecting a high-speed water jet into a water-filled chamber through a nozzle. When the cavitation bubbles approach the surface of the material, the sudden increase of the local pressure due to the huge turbulent pressure pulsation causes their collapse and generation of shock waves [13]. These shock waves act on the surface of the material, and propagate into the interior of the material, due to the high concentration of energy (the peak value of the collapse pressure reaches the gigapascal (GPa) range) [14]. The peak stress of the shock wave decreases as a shock wave propagates deeper into the material. When the peak value of the collapse pressure exceeds the Huguenot elastic limit (HEL) of the material, it yields and plastically deforms. The plastic deformation of the material continues until the peak stress falls below the dynamic yield strength. Since the loading direction is downward and the material is free on the bottom side, the material bends downward and fill the die cavity. The forming mechanism is similar to that of a punch forming by a laser-induced cavitation bubble. They all use the collapse of the cavitation bubble as a source force for the forming.

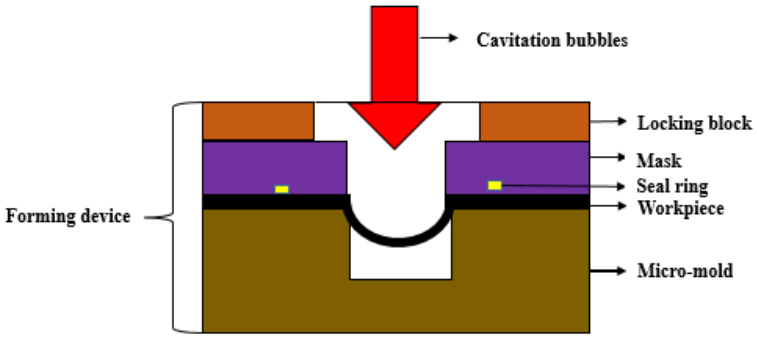

Fig. 1 Schematic of the water jet cavitation shock micro-bulging.

III. EXPERIMENTAL DETAILS

3.1 Material

In this experiment, a cold rolled 304 stainless steel foils were selected as the specimen due to their resistance to corrosion and excellent mechanical properties. Thus, 304 stainless steel foils with the thickness of 100 μm were cut into squares of 50 mm × 50 mm, in order to make this experiment possible. The 304 stainless steel foils squares were cleaned of dirt with anhydrous alcohol. Then, the residual liquid was wiped off the surface of the 304 stainless steel foils squares. In addition, to study the range of cavitation zone where the

International Journal of Engineering Applied Sciences and Technology, 2021
Vol. 6, Issue 6, ISSN No. 2455-2143, Pages 22-30
Published Online October 2021 in IJEAST (http://www.ijeast.com)

cavitation water jet acts on the surface of the sample, 8090Al-Li alloy with a low yield stress, high corrosion resistance, and low sensitivity at normal strain rate was selected as the sample for cavitation water jet shock strengthening experiment. The 8090Al-Li alloy sample with a thickness of 4 mm was cut into 50 mm × 50 mm by wire cutting. The sample was polished with 180 - 3000 mesh sandpaper. Then placed directly under the nozzle with a target distance of 120 mm. A high-definition camera was used to shoot the cavitation water jet influencing the sample. Table 1 and Table 2 shows the chemical composition and the mechanical properties of 304 stainless steel foils. The chemical composition and the mechanical properties of the 304 stainless steel foils is shown in table 1 and 2.

Table 1. The chemical composition of 304 stainless steel

Element	C	Mn	P	S	Si	Cr	Ni
Wt (%)	≤ 0.8	≤ 2.0	≤0.045	≤0.03	≤ 1.0	≤ 18.0	≤ 8.0

Table 2. The mechanical properties of 304 stainless steel

Elastic modulus (GPa)	Poisson ratio	Yield strength (MPa)	Tensile strength (MPa)	Extension rate (%)
194	0.3	≥ 205	≥ 520	≤ 40

3.3 Experimental setup

Figure 2 shows the experimental setup of the water jet cavitation shock micro bulging. Tap water was reserved for at least 20 hours before the test in a large tank of size 1.5 m × 2 m × 2.5 m, with a temperature of 24 ± 3 °C. The experiments are carried out using a water tank (transparent) having a height of 900 mm and a square horizontal cross-sectional area of 500 mm × 500 mm. Due to the visualization flow purpose, the tank is made of acrylic resin. The nozzle, which was designed with reference to the angular nozzle for generating the periodic behavior of the water jets cavitation [15] for this experiment, is as shown in Fig. 3. The ratio of the optimum size is d:L = 1:8 [16], where the throat diameter d of the nozzle is 1.5 mm, the throat length L is 12 mm. The nozzle was situated 160 mm deep from the surface of the water and the flow through the nozzle was driven using the plunger pump to generate the submerged cavitation jets in the high-pressure test cell. The diameter and the depth of the micro-die cavity are about 1.2 mm and 3 mm, respectively. The upstream and downstream pressure of the nozzle was measured by the pressure transducer. In the present paper, the pressures are absolute pressures. Although the maximum operating pressure of the plunger pump is 30 MPa, most of the experiments are carried out at 8-20 MPa. The blank holder force was 26 N, which can inhibit the radial flow of material. The standoff distance S is defined as the distance between the nozzle outlet and the surface of the specimen under test. In the present experiment, the target distance S is the distance between the nozzle outlet and the specimen and the eccentric distance SL is the axial distance between the cavity of the micro-die and the jet axis. Experimental condition is shown in table 3.

Table 3 The detailed experimental conditions.

Parameters	value
Pressure (P)	8MPa 12MPa 16MPa 20MPa
Standoff distance (S)	120mm
Time (t)	120sec
Die diameter (Ø)	1.2mm
Depth (h)	3mm
Nozzle angle (θ)	30°
Blank holder force (F)	26N

International Journal of Engineering Applied Sciences and Technology, 2021
Vol. 6, Issue 6, ISSN No. 2455-2143, Pages 22-30
Published Online October 2021 in IJEAST (http://www.ijeast.com)

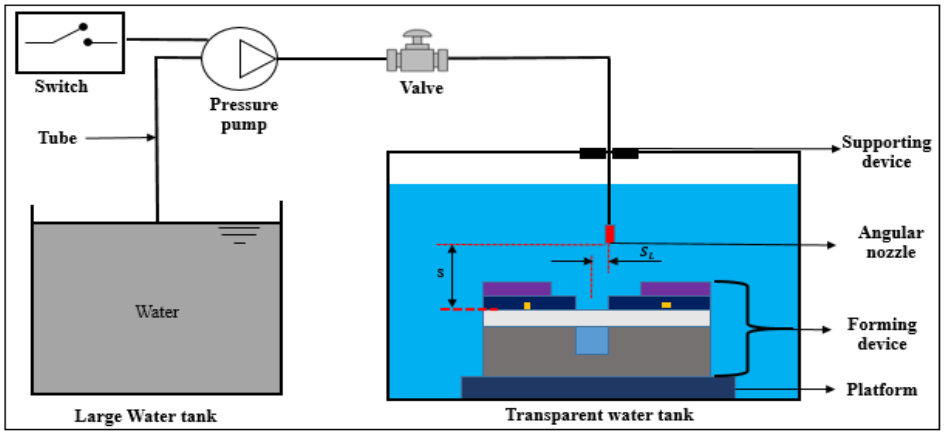

Fig. 2 Experimental system of water jet cavitation shock micro bulging.

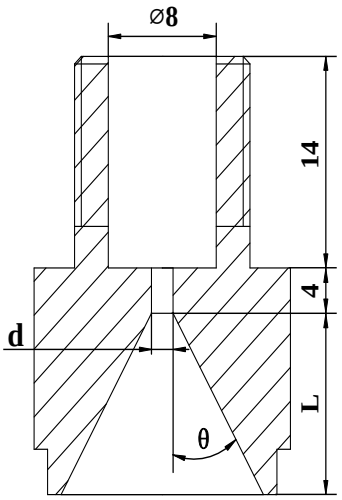

Fig. 3 Nozzle geometry diagram.

The cavitation number σ, which is an important parameter for the flow of the cavitation, is defined as a resistance measurement of the flow to cavitation [17, 18]. The pressure difference determines the flow speed between upstream and downstream pressures in the nozzles. Therefore, the cavitation number σ is denoted by:

$$\sigma = \frac{p_2}{p_1} \qquad (1)$$

where, $\boldsymbol{P_1}$ is the upstream (incident) pressure, $\boldsymbol{P_2}$ is the downstream pressure. Incident pressure is one of the important parameters in the process of water-jet cavitation shock micro bulging. The incident pressure $\boldsymbol{P_1}$ was set as 8, 12, 16 and 20 MPa while the downstream pressure $\boldsymbol{P_2}$ was maintained constant. Thus the cavitation number σ values were 0.0125, 0.0083, 0.0063 and 0.005 respectively. The test duration $\boldsymbol{t}$ was 2 min, and five samples were tested under each incident pressure.

IV. RESULTS AND DISCUSSIONS

The results presented in this article includes the formed sample and the effect of incident pressure on the cavitation zone range after the cavitation water jet processes.

4.1 Bulged sample

A 304 stainless steel foil with a size of 50 mm × 50 mm was selected for array micro-bulging experiments. Figure 4(a) is the macroscopic view of the surface of 304 stainless steel foil micro-bulged parts after the incident pressure P = 12 MPa, target distance S = 120 mm, and t = 120 sec. From the figure of the topography, you can see that, the bulged parts show different degrees of bulging effect. According to the analysis

International Journal of Engineering Applied Sciences and Technology, 2021
Vol. 6, Issue 6, ISSN No. 2455-2143, Pages 22-30
Published Online October 2021 in IJEAST (http://www.ijeast.com)

of the bulged surface of the micro-bulged sample. The shock zone of the cavitation water jet can be divided into three areas from the center to the periphery, firstly is the jet shock zone, which is a circular area within a certain range of the jet center, the radius R_1 was about 10.6 mm, the bulging depth of this area, is not large. Secondly, is the cavitation shock zone which is the annular area adjacent to the jet shock zone, the outer radius R_2 of the annular area was about 17.3mm, and the bulging effect of the micro-bulged parts was remarkable. Finally, is the outer ring shock zone which is the outermost area, the bulging effect of this area and the cavitation shock zone are different, and the bulging depth decreases rapidly. Figure 4(b) is the three-dimensional morphology cloud image of pit 2 in Figure 4(a). The cross-section shows a smooth outline. No cracks appeared on the surface of the bulged pit, and there were no conventional defects such as wrinkles around the bulged pit and good surface quality was obtained. Figure 4(c) is the bulging depth of the sample in Figure 4(a) in the direction of line P1. From the figure, it can be seen that the bulging depth of the outer ring shock zone and the bulging depth of the jet shock zone are not ideal, while the pits in the cavitation shock zone (that is, pits 2~4 and 10~12) obtained good geometric characteristics. Finally, the consistency of the maximum bulging depth was relatively good. The 304 stainless steel foil micro-bulged parts showed that the micro-pits in the cavitation shock zone had a large bulging depth and their uniformity was relatively good, indicating that the circular array feature micro-die has good performance in the cavitation water jet shock microforming process. The forming effect, which also shows that the cavitation water jet shock metallic foil micro-bulging process was very effective in array feature micro-bulging.

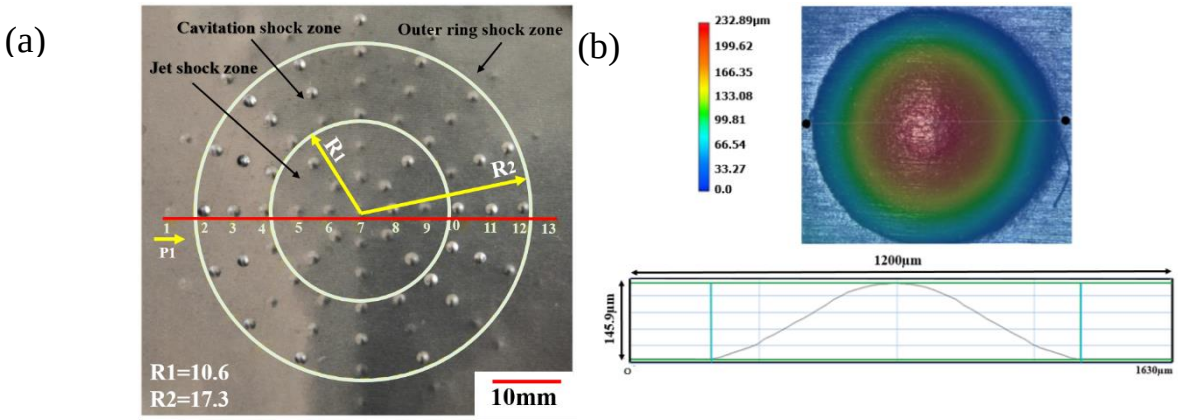

(a) Macroscopic morphology of the sample (b) Pit 2 three-dimensional morphology

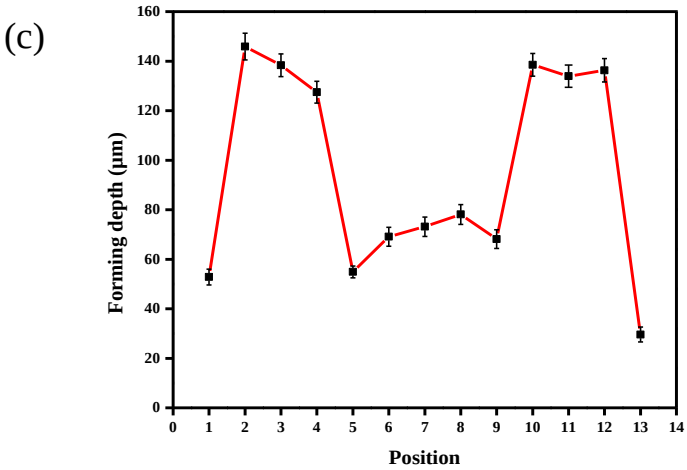

(c) The depth of the micro-pits in the P1 direction

Fig.4. Workpiece based on large-area array feature die

International Journal of Engineering Applied Sciences and Technology, 2021
Vol. 6, Issue 6, ISSN No. 2455-2143, Pages 22-30
Published Online October 2021 in IJEAST (http://www.ijeast.com)

In the jet shock zone, due to the blocking effect of the surrounding liquid, the velocity of the high-speed jet from the nozzle continues to decrease. Also due to the long target distance, when the droplet reaches the surface of the sample at a low velocity and it gives fewer cavitation bubbles. The impact force generated on the sample surface was relatively small. In the cavitation shock zone, the dynamic jet mixes with the surrounding static water to form a pressure gradient, and a vortex is generated at the boundary, forming a large number of cavitation bubbles above the sample. When the collapse occurs, the impact force on the surface of the sample shows the largest. A small amount of cavitation diffuses out of the cavitation shock zone to form an outer ring shock zone. This zone is far from the jet, and only a small amount of induced cavitation has a limited effect on the material [19]. The principle of the difference in the three-zone morphology of submerged cavitation water jets (Jet shock zone, cavitation shock zone, and outer ring shock zone) is shown in Figure 5.

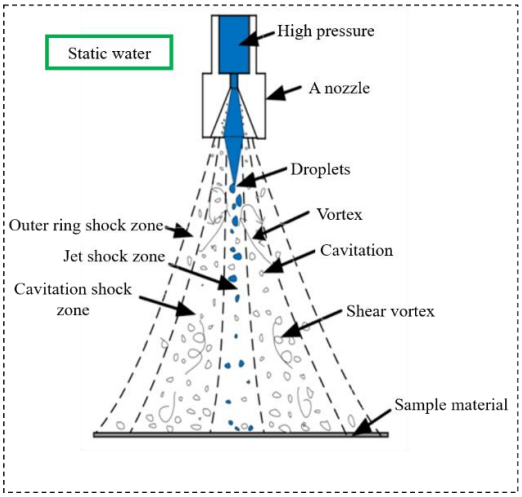

Fig. 5 Schematic diagram of submerged water-jet cavitation shock zone

4.2 Effect of incident pressure on the range of cavitation zone

To investigate the influence of the incident pressure on the width of the cavitation bulging zone. The experiment used a target distance of 120 mm and an impact time of 120 secs, varying the incident pressure (8, 12, 16, and 20 MPa) on the width range of the cavitation bulging zone of the 304 stainless steel foil bulged part, as shown in Figure 6. It can be observed from the figure that when the pressure was 8 MPa, the range of the cavitation bulging zone was 13.9 ~ 21.1 mm, also when the pressure was 12 MPa, the range of the cavitation bulging zone was 10.6 ~ 17.3 mm. At the time, when the pressure was 16 MPa, the range of cavitation bulging zone was 10.6 ～21.1 mm. In addition, when the pressure was 20 MPa, the range of the cavitation bulging zone was 3.5 ～21.1 mm. It can be seen that with the increase of incident pressure, the cavitation shock zone increases gradually and the width range of the cavitation bulging zone increases accordingly. This is because at the jet shock zone there was a blocking effect at the surrounding liquid, this makes the velocity of the high-speed jet from the nozzle continues to decrease. Also due to the long target distance, when the droplet reaches the surface of the sample at a low speed it produces fewer cavitation bubbles. This makes the impact force generated on the sample surface relatively small and produces lower pits especially when the pressure is low at 8 MPa. In the cavitation shock zone, the dynamic jet mixes with the surrounding static water to form a pressure gradient, and a vortex is generated at the boundary, forming a large number of cavitation bubbles above the sample. Then after the collapse has occurred, the impact force on the surface of the sample shows the largest even at the jet shock zone and increased beyond the outer ring shock zone when the pressure was increased to 20 MPa.

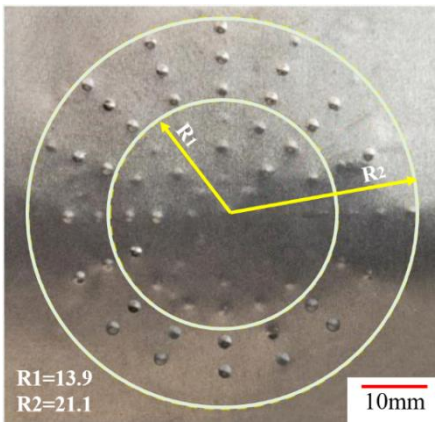

(a) 8MPa

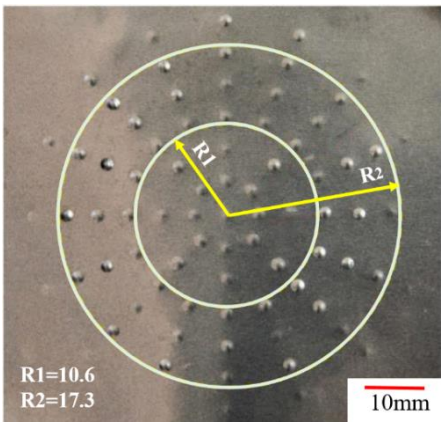

(b) 12MPa

International Journal of Engineering Applied Sciences and Technology, 2021
Vol. 6, Issue 6, ISSN No. 2455-2143, Pages 22-30
Published Online October 2021 in IJEAST (http://www.ijeast.com)

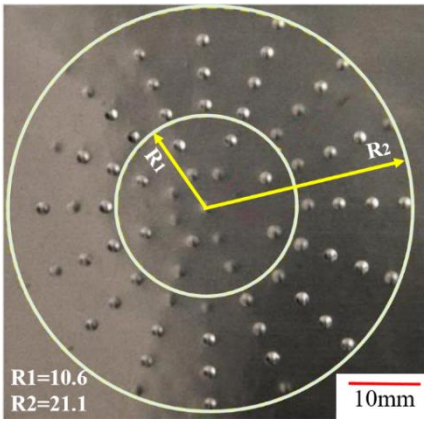

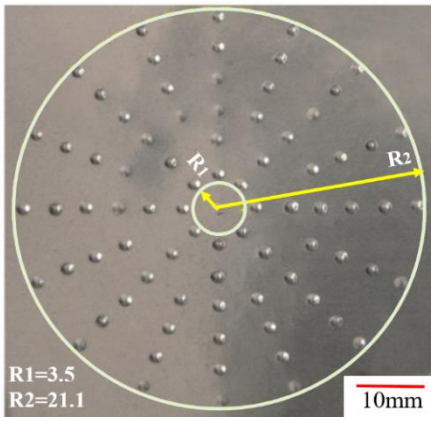

(c) 16MPa (d) 20MPa

Fig. 6 Macroscopic topography variation with incident pressures

Since the micro-pits on the sample surface had a diffuse reflection and showed a matte color, the distribution of the pits on the sample surface could be obtained. The incident pressure was adjusted to obtain the range of cavitation zone where the water jet acts on the surface of the 8090Al-Li alloy sample as shown in Figure 7. It can be seen from the figure that the surface of the 8090Al-Li alloy sample after the impact of the cavitation water jet had been strengthened, and a large number of pits were distributed in the strengthened area. To characterize the range of the cavitation shock zone of the cavitation water jet, the width of the strengthened area was used for characterization. From the figure, it can be seen that the width of the strengthened area changes with the change of the incident pressure, and was distributed in a ring shape. When the pressure was 8 MPa, the range of cavitation shock zone was 12.4 ～22.9 mm. Then when the pressure was 12 MPa, the range of cavitation shock zone was 8.8 ～19.4 mm. Again, when the pressure was 16 MPa, the range of cavitation shock zone was 9.8 ～23.5 mm. In addition, when the pressure was 20 MPa, the range of cavitation shock zone was 3.5 ～21.4 mm. Therefore, with the increase of incident pressure, the width of the cavitation shock zone gradually increased. Combined with the above array microforming experiments, under the same incident pressure, the cavitation impact forming zone was almost the same as the cavitation strengthening zone, which not only shows that the cavitation zone had a good forming effect, but also verifies the rationality of the array micro-die design.

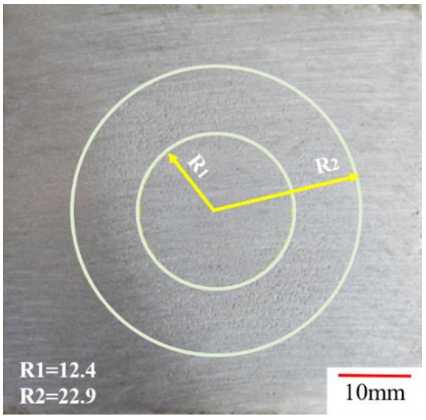

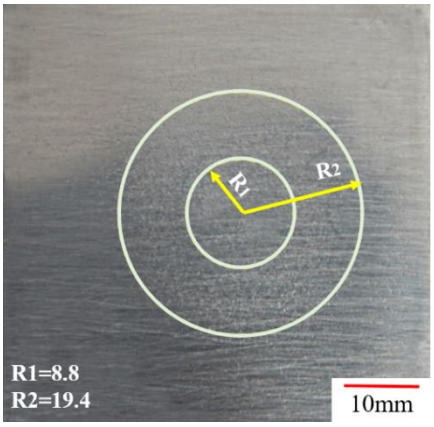

(a) 8MPa (b) 12MPa

International Journal of Engineering Applied Sciences and Technology, 2021
Vol. 6, Issue 6, ISSN No. 2455-2143, Pages 22-30
Published Online October 2021 in IJEAST (http://www.ijeast.com)

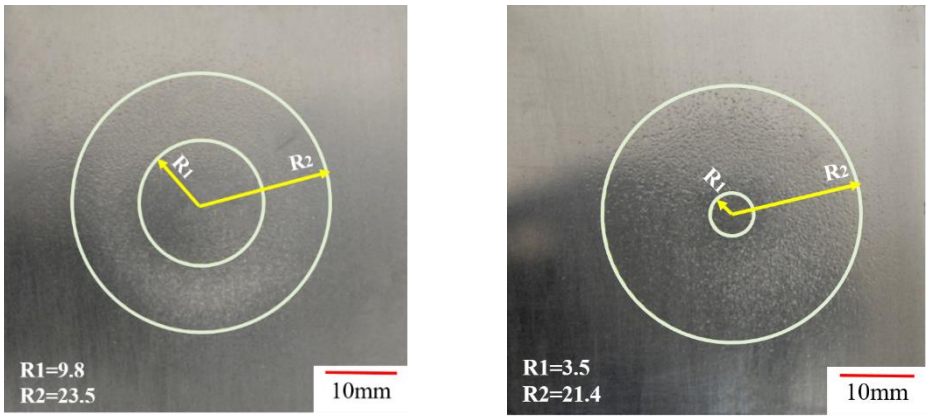

(c) 16MPa (d) 20MPa

Fig. 7. Variation of cavitation water jet shock field with incident pressure

V. CONCLUSION

This study presents the experiment of a cavitation water jet shock micro-bulging of 304 stainless steel foil and 8090Al-Li alloy strengthening. Base on the large area array characteristic micro-bulging experiment, the cavitation zone range and its influencing factors under the action of cavitation water jet are studied. Then the single characteristic micro-bulging experiment was carried out, and the impact micro-bulging law of cavitation water jet was analyzed and studied from the aspects of bulged sample and the effect of incident pressure on the range of cavitation zone of which the following conclusions were obtained. The processing method of cavitation water jet shock micro-bulging experiment of the formed metal foil results showed that the proposed new method could obtain the micro-bulged parts with good surface quality and relatively uniform impact depth bulged parts. With the effect of incident pressure on the range of cavitation zone, was found that the effective area of action of the cavitation water jet showed a ring. That is when the incident pressure was 20 MPa with a target distance of 120 mm, the maximum cavitation shock (bulging) zone showed rings of 3.5 ～21.1 mm with the 304 stainless steel foil and 3.5 mm~21.4 mm also with the 8090Al-Li alloy plate which were approximately same when the angular nozzle and cavitation system designed were used.

VI. REFERENCE

1 Brennen, C. E. (2014). *Cavitation and bubble dynamics*: Cambridge University Press.

2 FUJIKAWA, S., & AKAMATSU, T. (1978). Experimental investigations of cavitation bubble collapse by a water shock tube. *Bulletin of JSME, 21*(152), 223-230.

3 Geiger, M., Kleiner, M., Eckstein, R., Tiesler, N., & Engel, U. (2001). Microforming. *CIRP Annals, 50*(2), 445-462. doi: https://doi.org/10.1016/S0007-8506(07)62991-6

4 Jahan, M., Kakavand, P., Kwang, E., Rahman, M., & Wong, Y. (2015). An experimental investigation into the micro-electro-discharge machining behaviour of aluminium alloy (AA 2024). *The International Journal of Advanced Manufacturing Technology, 78*(5-8), 1127-1139.

5 Jiang, Z., Zhao, J., & Xie, H. (2017). Chapter 1 - Fundamentals of Microforming. In Z. Jiang, J. Zhao & H. Xie (Eds.), *Microforming Technology* (pp. 3-27): Academic Press.

6 Liu, H., Gong, J., Ma, Y., Cui, J., Li, M., & Wang, X. (2020). Investigation of novel laser shock hydroforming method on micro tube bulging. *Optics and Lasers in Engineering, 129*, 106073. doi: https://doi.org/10.1016/j.optlaseng.2020.106073

7 Liu, H., Sun, X., Shen, Z., Li, L., Sha, C., Ma, Y., . . . Wang, X. (2017). *Experimental and Numerical Simulation Investigation on Laser Flexible Shock Micro-Bulging* (Vol. 7).

8 Marcon, A., Melkote, S. N., Castle, J., Sanders, D. G., & Yoda, M. (2016). Effect of jet velocity in co-flow water cavitation jet peening. *Wear, 360-361*, 38-50. doi: https://doi.org/10.1016/j.wear.2016.03.027

9 Marcon, A., Melkote, S. N., & Yoda, M. (2018). Effect of nozzle size scaling in co-flow water cavitation jet peening. *Journal of Manufacturing Processes, 31*, 372-381. doi: https://doi.org/10.1016/j.jmapro.2017.12.002

10 Quaisie, J. K., Yun, W., Zhenying, X., Chao, Y., Li, F., Baidoo, P., . . . Asamoah, E. (2020). Experimental Study on Water-Jet Shock Microforming Process Using Different Incident

Pressures. *Advances in Materials Science and Engineering, 2020*.

11 Sato, K., Sugimoto, Y., & Ohjimi, S. (2009). Pressure-wave formation and collapses of cavitation clouds impinging on solid wall in a submerged water jet.

12 Sekyi-Ansah, J., Wang, Y., Quaisie, J. K., Li, F., Yu, C., Asamoah, E., & Liu, H. (2021). Surface Characteristics and Cavitation Damage in 8090Al–Li Alloy by Using Cavitation Water Jet Peening Processing. *Iranian Journal of Science and Technology, Transactions of Mechanical Engineering, 45*(1), 299-309.

13 Soyama, H. (2013). Effect of nozzle geometry on a standard cavitation erosion test using a cavitating jet. *Wear, 297*(1-2), 895-902.

14 Soyama, H. (2019). Comparison between the improvements made to the fatigue strength of stainless steel by cavitation peening, water jet peening, shot peening and laser peening. *Journal of Materials Processing Technology, 269*, 65-78. doi: https://doi.org/10.1016/j.jmatprotec.2019.01.030

15 Soyama, H., Yamauchi, Y., Adachi, Y., Sato, K., Shindo, T., & Oba, R. (1995). High-speed observations of the cavitation cloud around a high-speed submerged water jet. *JSME International Journal Series B Fluids and Thermal Engineering, 38*(2), 245-251.

16 Wang, C., Cheng, L., Liu, Y., & Zhu, C. (2020). Ultrasonic flexible bulging process of spherical caps array as surface texturing using aluminum alloy 5052 ultra-thin sheet. *Journal of Materials Processing Technology, 284*, 116725. doi: https://doi.org/10.1016/j.jmatprotec.2020.116725

17 Wang, X., Sun, K., Ma, Y., Shen, Z., Liu, F., & Liu, H. (2019). Experimental investigation on laser shock micro hydraulic bulging of copper foil. *Optics & Laser Technology, 115*, 390-397. doi: https://doi.org/10.1016/j.optlastec.2019.02.048

18 Wu, D., & Xie, H. (2017). A novel 3D deformation measurement method under optical microscope for micro-scale bulge-test. *Optics and Lasers in Engineering, 98*, 190-197. doi: https://doi.org/10.1016/j.optlaseng.2017.07.001

19 Yamauchi, Y. (1996). Suitable region of high-speed submerged water jets for cutting and peening. *International Journal of Multiphase Flow, 22*(S1), 135-135.